Inorganic Chemistry

ARTICLE

pubs.acs.org/IC

Syntheses and Crystal Structures of Two New Bismuth Hydroxyl Borates Containing $[Bi_2O_2]^{2+}$ Layers: $Bi_2O_2[B_3O_5(OH)]$ and $Bi_2O_2[BO_2(OH)]$

Rihong Cong,[†] Junliang Sun,[‡] Tao Yang,[†] Mingrun Li,[‡] Fuhui Liao,[†] Yingxia Wang,*[,†] and Jianhua Lin*[,†]

[†]Beijing National Laboratory for Molecular Sciences, State Key Laboratory of Rare Earth Materials Chemistry and Applications, College of Chemistry and Molecular Engineering, Peking University, Beijing 100871, P. R. China

[‡]Inorganic & Structural Chemistry and Berzelii Centre EXSELENT on Porous Materials, Stockholm University, SE-106 91 Stockholm, Sweden

Supporting Information

ABSTRACT: Two new bismuth hydroxyl borates, $Bi_2O_2[B_3O_5(OH)]$ (**I**) and $Bi_2O_2[BO_2(OH)]$ (**II**), have been synthesized under hydrothermal conditions. Their structures were determined by single-crystal and powder X-ray diffraction data, respectively. Compound **I** crystallizes in the orthorhombic space group *Pbca* with the lattice constants of a = 6.0268(3) Å, b = 11.3635(6) Å, and c = 19.348(1) Å. Compound **II** crystallizes in the monoclinic space group *Cm* with the lattice constants of a = 5.4676(6) Å, b = 14.6643(5) Å, c = 3.9058(1) Å, and β = 135.587(6)°. The borate fundamental building block (FBB) in **I** is a three-ring unit $[B_3O_6(OH)]^{4-}$, which connects one by one via sharing corners, forming an infinite zigzag chain along the a direction. The borate chains are further linked by hydrogen bonds, showing as a borate layer within the ab plane. The FBB in **II** is an isolated $[BO_2(OH)]^{2-}$ triangle, which links to two neighboring FBBs by strong hydrogen bonds, resulting in a borate chain along the a direction. Both compounds contain $[Bi_2O_2]^{2+}$ layers, and the $[Bi_2O_2]^{2+}$ layers combine with the corresponding borate layers alternatively, forming the whole structures. These two new bismuth borates are the first ones containing $[Bi_2O_2]^{2+}$ layers in borates. The appearance of $Bi_2O_2[BO_2(OH)]$ (**II**) completes the series of compounds $Bi_2O_2[BO_2(OH)]$, $Bi_2O_2CO_3$, and $Bi_2O_2[NO_3(OH)]$ and the formation of $Bi_2O_2[B_3O_5(OH)]$ provides another example in demonstrating the polymerization tendency of borate groups.

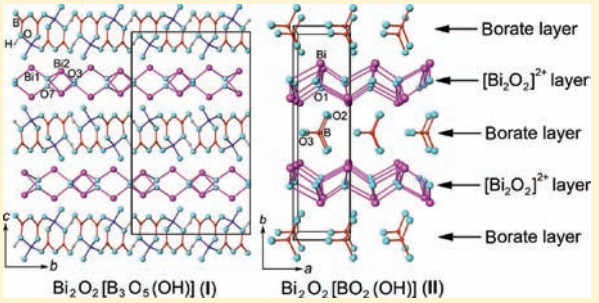

INTRODUCTION

Bismuth borates are of continuing interest due to their interesting linear and nonlinear optical (NLO) properties.[1−6] α-BiB_3O_6 (BIBO) is a well-known compound that exhibits excellent NLO properties,[5,6] of which the theoretical studies revealed that the NLO coefficients are mainly contributed by the heavily distorted $[BiO_4]^{5-}$ groups.[7] Besides BIBO, the known bismuth borates obtained from conventional solid-state reactions include $Bi_{24.5}BO_{38.25}$,[8] $Bi_4B_2O_9$,[9] $Bi_3B_5O_{12}$,[10] and $Bi_2B_8O_{15}$.[11−13] There are also two metastable compounds, $BiBO_3$ and $Bi_5B_3O_{12}$, crystallized from a Bi_2O_3−B_2O_3 melt.[14,15] Recently, remarkable progress has been made in the syntheses of new metal polyborates by applying nonconventional synthetic routes, such as boric acid flux, high-temperature/high-pressure, and hydrothermal methods.[16−18] $Bi[B_4O_6(OH)_2]OH$, BiB_2O_4F, $Bi_3[B_6O_{13}(OH)]$, and β- and γ-BiB_3O_6 were obtained by using boric acid as both reaction reagent and reaction medium,[19,20] while δ- and ε-BiB_3O_6 were realized under high pressures.[21,22]

In this paper, we present two new bismuth borates, $Bi_2O_2[B_3O_5(OH)]$ (**I**) and $Bi_2O_2[BO_2(OH)]$ (**II**), synthesized under hydrothermal conditions. These two new compounds possess a common structural feature: the intergrowth of borate layers and $[Bi_2O_2]^{2+}$ layers. In the literature, $[Bi_2O_2]^{2+}$ layers are usually observed in two well-known structure series: Aurivillius and Sillen phases.[23,24] The alternative stacking of $[Bi_2O_2]^{2+}$ layer and perovskite block leads to Aurivillius-phase with a general formula $[Bi_2O_2][A_{n-1}B_nO_{3n+1}]$, such as Bi_3NbTiO_9 (n = 2) and $Bi_4Ti_3O_{12}$ (n = 3).[23] If the interlayer units are halide or metal halide, these are the so-called Sillen-phases, such as BiOCl, $MBiO_2Cl$ (M = Ca, Pb, and etc).[24−26] In the present work, the structures of **I** and **II** can be understood in terms of the alternate stacking of $[Bi_2O_2]^{2+}$ layers with the anionic borate layers $[B_3O_5OH]^{2-}$ and $[BO_2(OH)]^{2-}$ respectively.

EXPERIMENTAL SECTION

Materials and Methods. The syntheses of $Bi_2O_2[B_3O_5(OH)]$ (**I**) and $Bi_2O_2[BO_2(OH)]$ (**II**) were carried out in closed Teflon autoclaves. The starting materials, H_3BO_3 and Bi_2O_3, are of analytical grade and

Received: February 23, 2011
Published: May 06, 2011

 © 2011 American Chemical Society

used as purchased without further purification. Typically, a mixture of 0.9000 g (1.931 mmol) of Bi_2O_3 and 1.9108 g (30.904 mmol) of H_3BO_3 with Bi/B ratio of $^1/_8$ was ground in an agate mortar and then transferred to a 25 mL Teflon autoclave. Then an appropriate amount of water was added, and the reaction was carried out at 220 °C for 3 days. The product was washed by hot distilled water (80 °C) and then dried at 80 °C. Phase **I** was obtained as yellowish block crystals with a yield of ~90% (based on Bi) when 9 mL of water was added; phase **II** formed in yellowish powder with a yield of ~85% if 12 mL of water was added. The products were highly sensitive to the content of water. If the added water was less than 9 mL, a mixture of $Bi_3B_5O_{12}$ and **I** formed; if between 9 and 12 mL, a mixture of **I** and **II** was obtained; if more than 12 mL, a dual-phase product of $Bi_4B_2O_9$ and **II** appeared.

Structure Analysis and Characterizations. A single crystal of **I** in the size of 0.09 × 0.08 × 0.07 mm^3 was used for the X-ray diffraction (XRD) data collection on a NONIUS Kappa-CCD using a graphite-monochromated Mo Kα radiation (λ = 0.71073 Å) at 293 K. A total of 17 869 reflections were collected in the region of 7.48° ≤ 2θ ≤ 56.54°, with −8 ≤ h ≤ 8, −15 ≤ k ≤ 15, −25 ≤ l ≤ 25, of which 1629 were independent and 1451 were observed ($I > 2\sigma$). Empirical absorption correction was applied.[27] The crystal structure was solved by direct methods (SHELXS-97) and refined by full-matrix least-squares refinement.[28] All the Bi, B, and O atoms were refined anisotropically. The hydrogen atoms were added in riding mode and refined isotropically. X-ray data collection conditions and the structure refinement results for $Bi_2O_2[B_3O_5(OH)]$ (**I**) are listed in Table S1 in Supporting Information.

Powder X-ray diffraction data for the structure analysis of **II** were collected at room temperature (25 °C) on a Bruker D8 Advance diffractometer in a transmission mode, using a curved germanium primary monochromated Cu Kα_1 radiation (λ = 1.54059 Å). The sample was supported by Mylar film, and the data in the 2θ range of 10−120° were collected in a step of 0.0197° with the remaining time 40 s per step under the tube conditions 40 kV and 40 mA.

Powder X-ray diffraction data of the samples after calcinations at different temperatures were collected on a Rigaku D/Max-2000 diffractometer using a rotating anode (Cu Kα, 40 kV and 100 mA), a graphite monochromator, and a scintillation detector. The elemental analyses of bismuth and boron were conducted by inductively coupled plasma method on a PROFILE SPEC atomic emission spectrometer, and the results showed the Bi/B molar ratios of 1:1.61 for **I** (the calculated value is 1:1.5) and 1.92:1 for **II** (the expected is 2:1). The combined thermogravimetric analysis (TGA) and differential scanning calorimetric (DSC) measurements were carried out on a Q600SDT thermogravimetric analyzer under nitrogen atmosphere with a heating rate of 10 °C/min from room temperature to 700 °C. FT-IR spectrum was measured on a NICOLET iN10 MX spectrum instrument. Solid-state ^{11}B MAS NMR experiment was recorded on a Varian Unity Plus-400 spectectrometer under a spinning speed of 20 kHz, using $BF_3 \cdot OEt_2$ as the standard material. Electron diffraction (ED) studies were performed on a JEOL JEM-2000 transmission electron miscroscope under 200 kV.

RESULTS AND DISCUSSION

Crystal Structure of $Bi_2O_2[B_3O_5(OH)]$ (I). Compound **I** crystallizes in an orthorhombic structure that contains 13 crystallographically independent non-hydrogen atoms, including two Bi, three B, and eight O. The atomic coordinates, isotropic thermal displacement factors, and BVS (bond valence sum) values for $Bi_2O_2[B_3O_5(OH)]$ (**I**) are listed in Table 1. The anisotropic temperature factors and the selected bond lengths and angles are provided in Tables S2 and S3, respectively, in Supporting Information. If only non-hydrogen atoms are taken into account, the chemical formula would be $[Bi_2B_3O_8]^-$. Obviously, one hydrogen atom is needed to compensate the negative charge. By analysis of the single-crystal XRD data, the hydrogen atom

Table 1. Atomic Coordinates, Isotropic Thermal Displacement Factors and BVS (Bond Valence Sum) Values for $Bi_2O_2[B_3O_5(OH)]$ (I)

atom	site	x	y	z	U_{eq}, Å^2	BVS
Bi1	8c	0.21213(8)	0.84609(4)	0.17776(2)	0.0072(2)	3.08
Bi2	8c	−0.20375(8)	0.09482(4)	0.19409(2)	0.0087(2)	2.94
O1	8c	−0.066(2)	0.9071(7)	0.1238(5)	0.012(2)	2.05
O2	8c	−0.198(2)	0.2605(8)	0.0856(5)	0.013(2)	2.01
O3	8c	0.090(2)	0.9851(7)	0.2423(4)	0.009(2)	2.28
O4	8c	0.113(2)	0.1444(7)	0.0858(4)	0.011(2)	2.06
O5	8c	0.4193(2)	0.0197(8)	0.0925(4)	0.015(2)	1.22
O6	8c	0.038(2)	0.7940(8)	0.0237(4)	0.013(2)	1.84
O7	8c	0.030(2)	0.7116(7)	0.2311(5)	0.012(2)	2.00
O8	8c	−0.263(2)	0.9354(7)	0.0175(5)	0.010(2)	1.74
B1	8c	−0.143(3)	0.848(1)	0.0626(7)	0.008(3)	3.09
B2	8c	0.269(2)	0.077(1)	0.0518(8)	0.008(3)	3.06
B3	8c	−0.046(2)	0.206(1)	0.0462(7)	0.007(3)	3.04
H	8c	0.51(2)	−0.01(1)	0.056(5)	0.023	

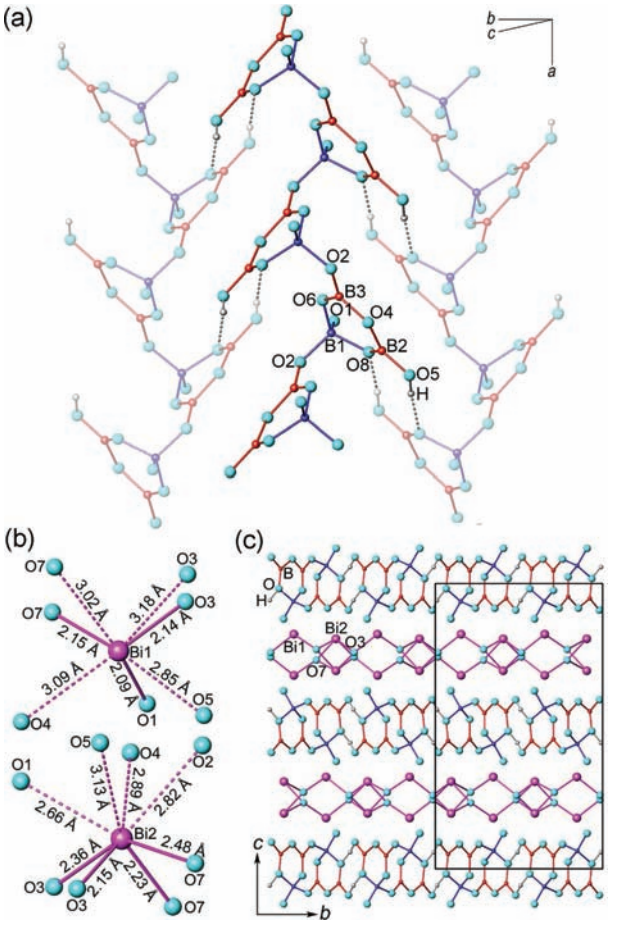

Figure 1. Structure of $Bi_2O_2[B_3O_5(OH)]$ (**I**): (a) the borate layer $[B_3O_5(OH)]^{2-}$; (b) coordination environments of Bi^{3+} ions; (c) projection along the a direction.

dx.doi.org/10.1021/ic200382b |*Inorg. Chem.* 2011, 50, 5098–5104

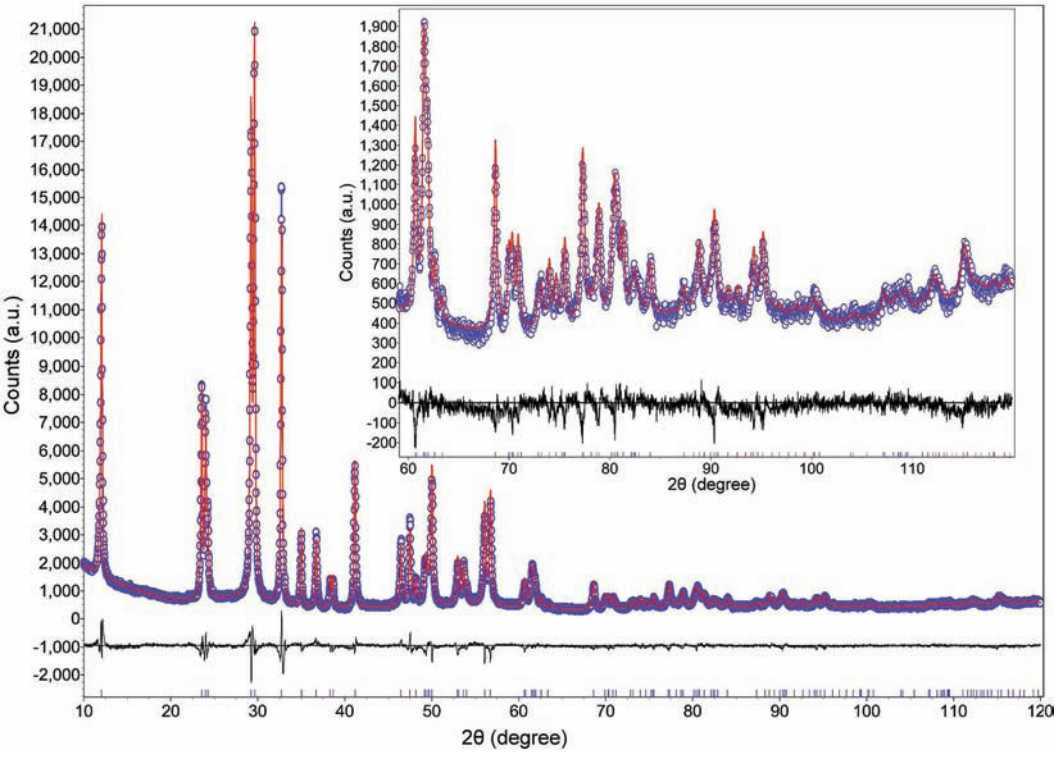

Figure 2. Rietveld refinement plot of the powder X-ray diffraction profile of $Bi_2O_2[BO_2(OH)]_5$ (**II**); the enlarged inset shows the good fit of the high-angle range. The circle symbol (○) represents the observed data, and the solid line is the calculated pattern; the difference curve is shown below the diffraction profile and the short vertical bars are the Bragg reflection positions.

was found to be close to O5 and was added in riding mode. The obviously low BVS value of 1.22 for O5 confirms that O5 is protonated. Its neighboring oxygen O8 also shows a relatively low BVS value of 1.74, indicating the existence of a hydrogen bond O5−H···O8 between them.

As shown in Figure 1a, B1 is coordinated by O1, O2, O6, and O8, forming a BO_4 tetrahedron; B2 locates at the center of three oxygen atoms, O4, O5, and O8, presenting as a $BO_2(OH)$ triangle; B3 is surrounded by O2, O4, and O6, also being a BO_3 triangle. All the bond distances and angles are in the normal ranges, and the bond lengths are 1.34−1.41 Å for those related to the BO_3 group and 1.44−1.51 Å in the BO_4 group (Table S3, Supporting Information). These three borate groups connect to one another by sharing corners, forming a three-membered ring fundamental building block (FBB), $[B_3O_6(OH)]^{4-}$, which can be expressed as 3:$[(3{:}2\Delta + T)]$.[29,30] This kind of three-ring FBB is common in polyborates.[31,32] The FBBs are further connected by sharing corners (O2 atoms), resulting in an infinite zigzag chain along the *a* direction, as shown in Figure 1a. The main chain comprises the alternating connection of $B(1)O_4$ and $B(3)O_3$, while $B(2)O_2(OH)$ triangles appear as side branches with terminal OH groups. These OH groups cross-link the adjacent chains via hydrogen bonds (O5−H···O8), giving rise to a two-dimensional (2D) polyborate layer.

As shown in Figure 1b, Bi1 is hepta-coordinated and Bi2 is octa-coordinated with the Bi−O distances in the range of 2.09−3.17 Å. These irregular BiO_7 and BiO_8 polyhedra share edges in a 2D fashion. A fluctuant square $[Bi_2O_2]^{2+}$ layer can be visualized (Figure 1c), if Bi^{3+} and O3 and O7 atoms, which have no linkages to boron atoms, are taken into account. The structure of **I** can be therefore described as an alternate stacking of the cationic $[Bi_2O_2]^{2+}$ layers with the anionic $[B_3O_5(OH)]^{2-}$ layers along the *c* direction. The feature of the $[Bi_2O_2]^{2+}$ layers will be discussed later.

Crystal Structure of $Bi_2O_2[BO_2(OH)]$ (II). Since no single crystal suitable for the structure determination was obtained, the structure of **II** was solved by the powder X-ray diffraction (XRD) in combination with electron diffraction (ED). The ED patterns are shown in Figure S1 in Supporting Information, which initially could be indexed by a tetragonal lattice with parameters $a = b =$ 3.79 Å and $c = 14.1$ Å, while the indexing of the powder XRD pattern by PowderX[33] suggested a monoclinic unit cell, $a =$ 3.9060 Å, $b = 14.6657$ Å, $c = 3.8266$ Å, and $\beta = 89.98°$. Apparently, the above two sets of parameters are closely related. Due to the higher accuracy of powder XRD than ED, the monoclinic lattice was applied. It is found afterward that the monoclinic space group is a right choice. The pseudotetragonal symmetry in the ED images is due to the tetragonal distribution of Bi atoms that show strong scattering abilities for electrons; however, the distribution of triangular borate groups cannot comply with the tetragonal symmetry. The systematic absences of the peaks ($h + k + l = 2n + 1$) in the powder XRD profile suggest a body-centered lattice. In order to take a standard setting of space group, the original monoclinic cell was then transferred to a *C*-centered lattice with the refined parameters of $a =$ 5.4676(6) Å, $b = 14.6643(5)$ Å, $c = 3.9058(1)$ Å, and $\beta =$ 135.587(6)°. The possible space groups were *C*2, *Cm*, and *C*2/*m*. Because of the existence of $BO_2(OH)$ groups in the compound, the space group *Cm* was applied in the structure determination, though the $[Bi_2O_2]^{2+}$ layers, especially the heavy Bi^{3+}, could be related by inversion centers. The structure model was initially established by direct methods using the program EXPO,[34,35] and

dx.doi.org/10.1021/ic200382b |*Inorg. Chem.* 2011, 50, 5098–5104

Table 2. Atomic coordinates, Thermal Displacement Factors and Bond Valence Sum (BVS) Values for $Bi_2O_2[BO_2(OH)]$ (II)

atom	site	*x*	*y*	*z*	U_{eq}, Å^2	BVS
Bi	4*b*	0.9800	0.33774(7)	0.024(4)	[a]	3.19
B	2*a*	0.04(2)	0	0.11(4)	0.01(2)	2.98
O1	4*b*	0.95(1)	0.2575(9)	0.57(1)	0.031(9)	2.39
O2	4*b*	0.100(5)	0.918(1)	0.010(7)	0.054(8)	1.59
O3	2*a*	0.840(6)	0	0.213(8)	0.054(8)	1.28

[a] Anisotropic thermal displacement factors of Bi atom are U_{11} = 0.029(2), U_{22} = 0.089(3), U_{33} = 0.046(6), U_{23} = 0.005(6), U_{13} = 0.025(4), and U_{12} = −0.007(5) Å^2.

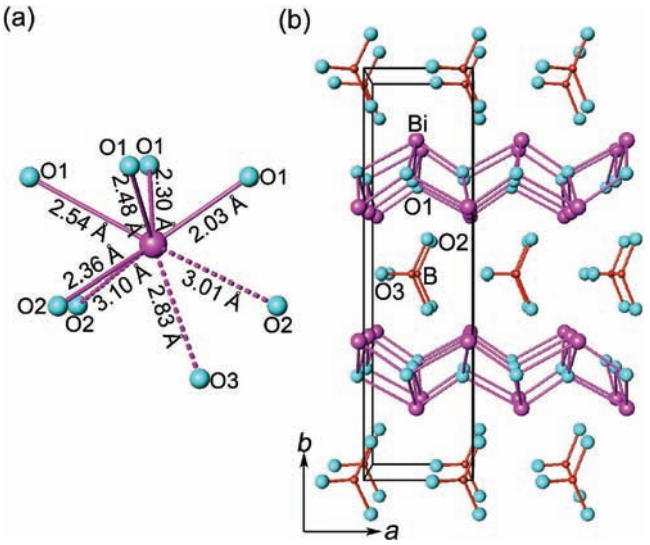

Figure 3. Structure of $Bi_2O_2[BO_2(OH)]$ (**II**): (a) coordination environment of Bi^{3+}; (b) projection along the *c* direction.

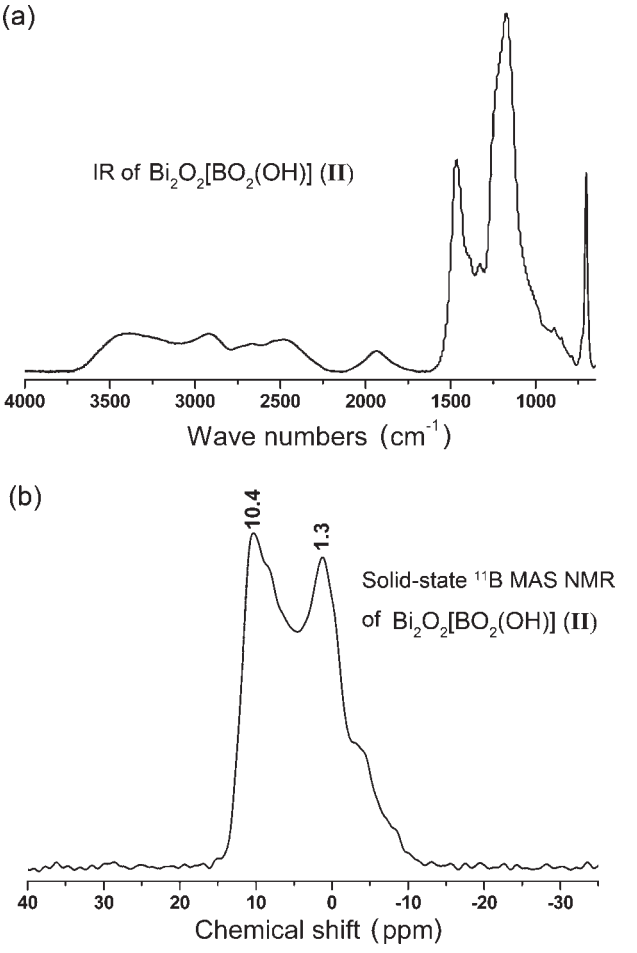

Figure 4. (a) IR and (b) solid-state ^{11}B MAS NMR spectrum for $Bi_2O_2[BO_2(OH)]$ (**II**).

one bismuth atom and one oxygen atom were located at this stage. Then the simulated annealing technique was applied using the program TOPAS and rigid bodies were defined for the borate groups.[36] All the atoms were revealed, and the Rietveld refinement of the structure was performed with the soft restraints on the thermal displacement parameters and B−O bond distances. During the refinement, the thermal displacement parameters of Bi atom were refined anisotropically, while those for other atoms were done isotropically. The Rietveld refinement was converged to *Rp* = 0.053 and *Rwp* = 0.070, and the plot is shown in Figure 2. The atomic coordinates, the thermal displacement factors, and the bond valence sums of each atom for **II** are listed in Table 2. The data collection conditions and structure refinement results for $Bi_2O_2[BO_2(OH)]$ (**II**) are summarized in Table S4 in Supporting Information. The selected bond distances and angles are provided in Table S5 in Supporting Information.

There are five crystallographically independent non-hydrogen atoms in **II**, including one Bi, one B, and three O, in which B and O3 atoms are located on the mirror plane (2*a* site), and others are located in general positions (4*b* site). As shown in Figure 3a, the bismuth atom is coordinated by eight oxygen atoms in an irregular environment with the normal bond lengths and angles (Table S5, Supporting Information), and the boron atom is coordinated by three oxygen atoms (two O2 and one O3) in a regular triangular environment. The triangular coordination of B is confirmed by IR and solid-state ^{11}B MAS NMR spectra (Figure 4). The absorption bands in the range of 1500−1100 cm^{-1} in IR are related to the vibrations of the BO_3 group (Figure 4a),[37] and the broad band peaking at 10.4 and 1.3 ppm in the solid-state ^{11}B MAS NMR spectrum (Figure 4b) is typical for the 3-fold coordinated boron atoms.[38]

The hydrogen-free formula is $[Bi_2BO_5]^-$. Apparently one hydrogen atom is needed to compensate the negative charge. It is difficult to determine the positions of hydrogen atoms directly from powder XRD data; however, the bond valences of oxygen atoms are helpful for the location of the hydrogen atoms. The oxygen atoms in the structure can be divided into two groups: one is O1 that only coordinates to four bismuth atoms; and the other includes O2 and O3, which connect to both bismuth and boron atoms. The bond valences of O2 and O3 are 1.59 and 1.28, respectively, which are significantly lower than 2, indicating the presence of a hydrogen bond between them. The distance between O2 and O3 in the structure of **II** is 2.61 Å, which is generally related to a strong hydrogen bond.[39] The borate FBB in **II** is the isolated $BO_2(OH)$ group, which connects to two adjacent FBBs by strong hydrogen bonds, appearing as a "borate layer" in the structure. These borate groups further share oxygen atoms with BiO_8 polyhedra. Similar to the situation in the structure of **I**, $[Bi_2O_2]^{2+}$ layers can be isolated from the structure

dx.doi.org/10.1021/ic200382b |*Inorg. Chem.* 2011, 50, 5098–5104

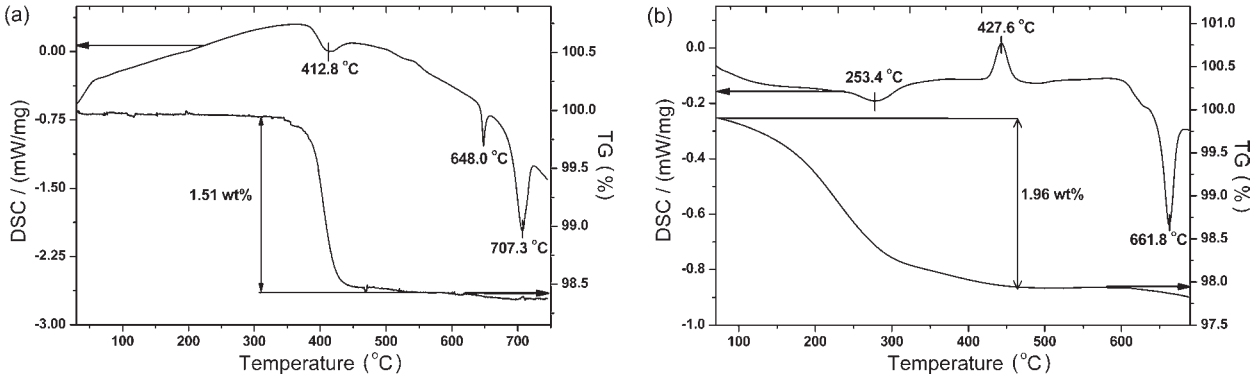

Figure 5. TGA−DSC curves of (a) $Bi_2O_2[B_3O_5(OH)]$ (**I**) and (b) $Bi_2O_2[BO_2(OH)]$ (**II**).

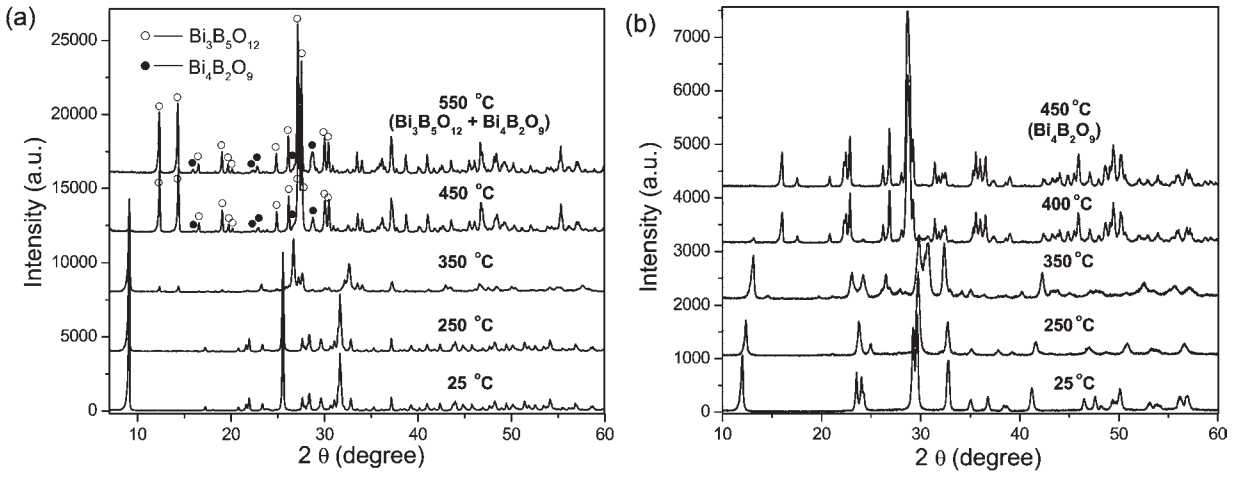

Figure 6. X-ray diffraction patterns of the as-synthesized and the calcined products at different temperatures for (a) $Bi_2O_2[B_3O_5(OH)]$ (**I**) and (b) $Bi_2O_2[BO_2(OH)]$ (**II**).

of **II**, as shown in Figure 3b. Then the structure of **II** can be described as cationic $[Bi_2O_2]^{2+}$ layers connected by interlayer $[BO_2(OH)]^{2-}$ groups along the *b* direction.

Thermal Stability. Both **I** and **II** contain hydroxyl groups, and their thermal gravimetric analyses (TGA) present weight changes corresponding to the dehydration process, as shown in Figure 5. Compound **I** shows a weight loss of about 1.51 wt % between 350 and 500 °C due to the dehydration of the hydroxyl groups (calcd 1.55 wt %), accompanied by an endothermic peak at 412.8 °C on the DSC curve (Figure 5a). Compound **II** loses about 1.96% weight continuously from room temperature to about 460 °C (Figure 5b). According to the formula $Bi_2O_2[BO_2(OH)]$, the calculated weight loss corresponding to the dehydration of the hydroxyl groups is 1.77 wt %, and the 0.19% excess weight loss observed may be due to absorbed water. There are also other peaks at higher temperature on the DSC curves. In order to assign these peaks and understand the thermal behavior of **I** and **II**, the as-synthesized **I** and **II** were heated at different temperatures each for 10 h, and the powder XRD data of the calcined products were recorded at room temperature and are shown in Figure 6.

It can be seen that **I** retains its structure up to 250 °C (Figure 6a). It starts to dehydrate at 350 °C and then decomposes to a mixture of $Bi_4B_2O_9$ and $Bi_3B_5O_{12}$, which corresponds to the first endothermic peak at 412.8 °C on the DSC curve. According to the phase diagram of $Bi_2O_3-B_2O_3$ in the literature,[40] the second peak on the DSC curve (648.0 °C) coincides with the melting of the eutectic mixture of $Bi_4B_2O_9$ and $Bi_3B_5O_{12}$, and the third one (707.3 °C) corresponds to the point at the liquidus curve on the diagram.

For **II**, two endothermic peaks (253.4 and 661.8 °C) and one exothermic peak (427.6 °C) appeared in the DSC curve. As shown in Figure 6b, the structure of **II** is maintained until 350 °C and then collapses with the removal of hydroxyl groups. The exothermic peak at 427.6 °C corresponds to the formation of $Bi_4B_2O_9$ and the last endothermic peak at 661.8 °C is close to the melting point (675 °C) of $Bi_4B_2O_9$.[41]

$[Bi_2O_2]^{2+}$ Layers in the Structures of $Bi_2O_2[B_3O_5(OH)]$ (I) and $Bi_2O_2[BO_2(OH)]$ (II). $[Bi_2O_2]^{2+}$ layers have been found in two famous series: the Aurivillius phases and the Sillen phases.[23,24] The intergrowth fusion of $[Bi_2O_2]^{2+}$ layers with borate groups in **I** and **II** are similar to those in Sillen phases.[24−26] In addition, bismuth hydroxynitrates, $Bi_2O_2(OH)(NO_3)$, and oxycarbonates, $Bi_2O_2CO_3$, were also reported to have Sillen phase related structures.[42,43] The structure of $Bi_2O_2CO_3$ is shown in Figure S2 (Supporting Information). The $[Bi_2O_2]^{2+}$ layer in compound **II** is regular (Figure 7a), but the $[Bi_2O_2]^{2+}$ layer in compound **I** is severely distorted (Figure 7b). Usually, the Bi−O bonds within the $[Bi_2O_2]^{2+}$ layer are relatively short (less than 2.6 Å) in BiO_n polyhedron. For instance, in $Bi_2O_2CO_3$,

dx.doi.org/10.1021/ic200382b |*Inorg. Chem.* 2011, 50, 5098–5104

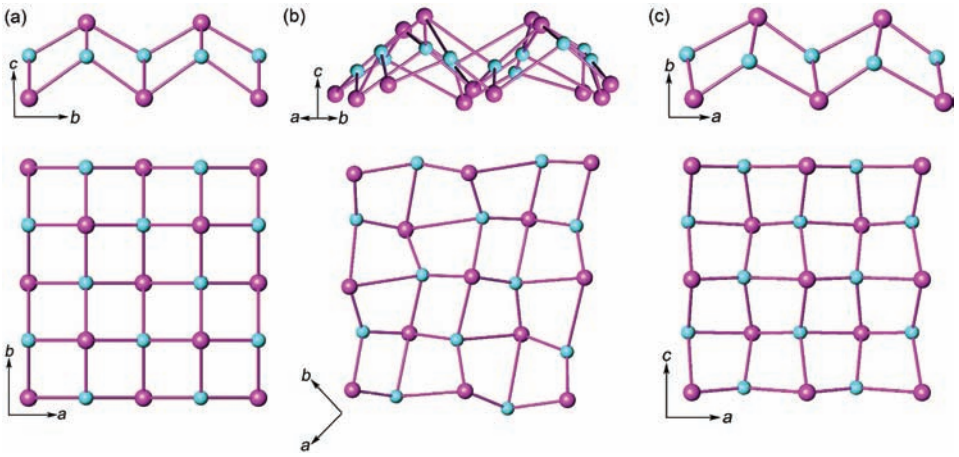

Figure 7. $[Bi_2O_2]^{2+}$ layers in the structures of (a) $Bi_2O_2CO_3$, (b) $Bi_2O_2[B_3O_5(OH)]$ (**I**), and (c) $Bi_2O_2[BO_2(OH)]$ (**II**).

the Bi^{3+} cation has four short and four long Bi−O bonds (Figure S2 in Supporting Information). In $Bi_2O_2[BO_2(OH)]$ (**II**), the Bi^{3+} cation links to oxygen atoms by five short and three long Bi−O bonds (Figure 3), and then the lone electron pair of Bi^{3+} faces toward the open space around Bi^{3+}, that is, the upper and lower sides of the $[Bi_2O_2]^{2+}$ layers. In $Bi_2O_2[B_3O_5(OH)]$ (**I**), the location of the lone electron pair of Bi^{3+} is different. Compound **I** contains two independent Bi^{3+} atoms: Bi1 and Bi2. Figure S3 in Supporting Information highlights the short bonds of BiO_n polyhedra. The coordination of Bi2 is only slightly distorted and is similar to that in regular $[Bi_2O_2]^{2+}$ layer. Bi1 is coordinated by seven oxygen atoms with three short and four long bonds (Figure 1b), and the open space around Bi1 is no longer upward or downward (Figure S3, Supporting Information). Instead, the O1 atom that links to B1 also coordinates to Bi1 by a short bond (2.09 Å). The insertion of this O1 atom then "pulls" the Bi1 atoms out of the $[Bi_2O_2]^{2+}$ layer and "pushes" the lone pair electrons of Bi^{3+} to the left or right side of the Bi1 cation.

Another interesting thing is to compare the formation of the series of bismuth compounds $Bi_2O_2[BO_2(OH)]$ (**II**), $Bi_2O_2CO_3$, and $Bi_2O_2[NO_3(OH)]$. From the view of the structural aspect, BO_3^{3-}, CO_3^{2-}, and NO_3^- are isoelectronic species that have a similar planar triangular structure, and as a consequence they may exist in solid-state compounds in a similar manner. Since these three entities have different negative charges, they may form the comparable compounds in different ways: the direct combination of $[Bi_2O_2]^{2+}$ with CO_3^{2-}, the combination of $[Bi_2O_2]^{2+}$ with BO_3^{3-} by the aid of a positive proton, and the formation of $Bi_2O_2[NO_3(OH)]$ by the involvement of a negative hydroxyl group. On the other side, both CO_3^{2-} and NO_3^- generally exist in compounds as isolated groups, but the borate group can be further polymerized. Therefore, we get an additional bismuth borate $Bi_2O_2[B_3O_5(OH)]$ (**I**), in which the polynuclear anion is an infinite zigzag chain formed by a three-ring unit $B_3O_5(OH)^{2-}$.

CONCLUSION

Two new bismuth hydroxyl borates, $Bi_2O_2[B_3O_5(OH)]$ (**I**) and $Bi_2O_2[BO_2(OH)]$ (**II**), were synthesized under hydrothermal conditions. The structures of **I** and **II** were solved by single-crystal and powder XRD data, respectively. The borate FBB in **I** is a three-ring unit, $[B_3O_6(OH)]^{4-}$, which connects to two adjacent FBBs by corner-sharing, forming an infinite zigzag chain with terminal hydroxyl groups. The chains link one another by hydrogen bonds, producing borate layers within the *ab*-plane. The FBB in **II** is an isolated $[BO_2(OH)]^{2-}$ triangle, which further connects to two neighboring FBBs by strong hydrogen bonds. The IR and solid-state ^{11}B MAS NMR spectra confirm the exclusive existence of BO_3 triangles in these structures. Compound **I** dehydrates at about 350 °C and decomposes to a mixture of $Bi_4B_2O_9$ and $Bi_3B_5O_{12}$, and compound **II** changes to $Bi_4B_2O_9$ at about 400 °C. These two new hydrous bismuth borates are the first examples of borates containing $[Bi_2O_2]^{2+}$ layers. The $[Bi_2O_2]^{2+}$ layers combine with the corresponding borate layers in an alternate stacking sequence in a similar manner as that in Sillen phases. The appearance of $Bi_2O_2[BO_2(OH)]$ (**II**) completes the series of inorganic compounds $Bi_2O_2[BO_2(OH)]$, $Bi_2O_2CO_3$, and $Bi_2O_2[NO_3(OH)]$, and the formation of $Bi_2O_2[B_3O_5(OH)]$ (**I**) provides another example in demonstrating the polymerization tendency of borate groups.

ASSOCIATED CONTENT

Supporting Information. CIF file of $Bi_2O_2[B_3O_5(OH)]$ (**I**), X-ray data collection conditions and crystallographic and structure refinement parameters for **I**, anisotropic thermal displacement factors for **I**, selected bond lengths and angles of **I**, X-ray data collection conditions and crystallographic and structure refinement parameters for $Bi_2O_2[BO_2(OH)]$ (**II**), selected bond lengths and angles for **II**, ED patterns of **II**, projection of the structure of $Bi_2O_2CO_3$ along the *b* direction and the coordination environment of Bi^{3+}, and highlighting of the short Bi−O bonds (<2.6 Å) in $[Bi_2O_2]^{2+}$ layer in **I**. This material is available free of charge via the Internet at http://pubs.acs.org.

AUTHOR INFORMATION

Corresponding Author

*E-mail: wangyx@pku.edu.cn, jhlin@pku.edu.cn. Tel: 86-10-62751715, 86-10-62755538. Fax: (86)1062753541.

Funding Sources

This work is financially supported by the State Science and Technology Commission of China (Grant 2010CB833103) and National Natural Science Foundation of China (Grant NSFC 20821091).

REFERENCES

(1) Becker, P. *Cryst. Res. Technol.* **2003**, *38*, 74–82.
(2) Opera, I.-I.; Hesse, H.; Betzler, K. *Opt. Mater.* **2004**, *26*, 235–237.
(3) Muehlberg, M.; Burianek, M.; Edongue, H.; Poetsch, Ch. *J. Cryst. Growth* **2002**, *237−239*, 740–744.
(4) Becker, P.; Held, P. *Cryst. Res. Technol.* **2001**, *36*, 1353–1356.
(5) Becker, P.; Liebertz, J.; Bohatý, L. *J. Cryst. Growth* **1999**, *203*, 149–155.
(6) Hellwig, H.; Liebertz, J.; Bohatý, L. *Solid State Commum.* **1999**, *109*, 249–251.
(7) Lin, Z. S.; Wang, Z. Z.; Chen, C. T.; Lee, M. H. *J. Appl. Phys.* **2001**, *90*, 5585–5590.
(8) Burianek, M.; Held, P.; Mühlberg, M. *Cryst. Res. Technol.* **2002**, *37*, 785–796.
(9) Hyman, A.; Perloff, A. *Acta Crystallogr.* **1972**, *B28*, 2007–2011.
(10) Vegas, A.; Cano, F. H.; Garcia-Blanco, S. *J. Solid State Chem.* **1976**, *17*, 151–155.
(11) Fröhlich, R.; Bohatý, L.; Liebertz, J. *Acta Crystallogr.* **1984**, *C40*, 343–344.
(12) Teng, B.; Yu, W. T.; Wang, J. Y.; Cheng, X. F.; Dong, S. M.; Liu, Y. G. *Acta Crystallogr.* **2002**, *C58*, i25–i26.
(13) Bubnova, R. S.; Alexandrova, J. V.; Krivovichev, S. V.; Filatov, S. K.; Egorysheva, A. V. *J. Solid State Chem.* **2010**, *183*, 458–464.
(14) Kargin, Yu. F.; Zhereb, V. P.; Egorysheva, A. V. *Russ. J. Inorg. Chem.* **2002**, *47*, 1240–1242.
(15) Becker, P.; Fröhlich, R. *Z. Naturforsch.* **2004**, *59b*, 256–258.
(16) Ivanova, A. G.; Belokoneva, E. L.; Dimitrova, O. V.; Mochenova, N. N. *Russ. J. Inorg. Chem.* **2006**, *51*, 584–588.
(17) Jing, J.; Lin, J. H.; Li, G. B.; Yang, T.; Li, H. M.; Liao, F. H.; Loong, C.-K.; You, L. P. *Angew. Chem., Int. Ed.* **2003**, *42*, 5607–5610.
(18) Huppertz, H.; von der Eltz, B. *J. Am. Chem. Soc.* **2002**, *124*, 9376–9377.
(19) Li, L. Y.; Li, G. B.; Wang, Y. X.; Liao, F. H.; Lin, J. H. *Chem. Mater.* **2005**, *17*, 4174–4180.
(20) Li, L. Y.; Li, G. B.; Wang, Y. X.; Liao, F. H.; Lin, J. H. *Inorg. Chem.* **2005**, *44*, 8243–8248.
(21) Knyrim, J. S.; Becker; Johrendt, P. D.; Huppertz, H. *Angew. Chem., Int. Ed.* **2006**, *45*, 8239–8241.
(22) Dinnebier, R. E.; Hinrichsen, B.; Lennie, A.; Jansen, M. *Acta Crystallogr.* **2009**, *B65*, 1–10.
(23) Aurivillius, B. *Ark. Kemi* **1949**, *1*, 463–471.
(24) Sillen, L. G. *Naturwissenschaften* **1942**, *30*, 318–324.
(25) Charkin, D. O.; Dytyatiev, O. A.; Dolgikh, V. A.; Lightfoot, P. *J. Solid State Chem.* **2003**, *173*, 83–90.
(26) Charkin, D. O.; Berdonosov, P. S.; Moisejev, A. M.; Shagiakhmetov, R. R.; Dolgikh, V. A.; Lightfoot, P. *J. Solid State Chem.* **1999**, *147*, 527–535.
(27) Blessing, R. H. *Acta Crystallogr.* **1995**, *A51*, 33–38. *J. Appl. Crystallogr.* **1997**, *30*, 421–426.
(28) Sheldrick, G. M. SHELXS 97, Program for the solution of Crystal Structures, and SHELXL 97, Program for the Refinement of Crystal Structures; University of Göttingen, Göttingen, Germany, 1997.
(29) Christ, C. L.; Clark, J. R. *Phys. Chem. Miner.* **1977**, *2*, 59–87.
(30) Burns, P. C.; Grice, J. D.; Hawthorne, F. C. *Can. Mineral.* **1995**, *22*, 1131–1151.
(31) Touboul, M.; Bois, C.; Mangin, D.; Amoussou, D. *Acta Crystallogr.* **1983**, *C39*, 685–689.
(32) Corazza, E.; Menchetti, S.; Sabelli, C. *Acta Crystallogr.* **1975**, *B31*, 1993–1997.
(33) Dong, C. *J. Appl. Crystallogr.* **1999**, *32*, 838–839.
(34) Altomare, A.; Cascarano, G.; Giacovazzo, C.; Guagliardi, A.; Burla, M. C.; Polidori, G.; Camalli, M. *J. Appl. Crystallogr.* **1994**, *27*, 1045–1050.
(35) Altomare, A.; Burla, M. C.; Cascarano, G.; Giacovazzo, C.; Guagliardi, A.; Moliterni, A. G. G.; Polidori, G. *J. Appl. Crystallogr.* **1995**, *28*, 842–846.
(36) TOPAS V2.1: General Profile and Structure Analysis Software for Powder Diffraction Data; Bruker AXS, Karlsruhe, Germany.
(37) Laperches, J. P.; Tarte, P. *Spectrochim. Acta* **1966**, *22*, 1201–1205.
(38) Li, J.; Xia, Sh. P.; Gao, Sh. Y. *Spectrochim. Acta* **1995**, *51*, 519–532.
(39) Emsley, J. *Chem. Soc. Rev.* **1981**, *9*, 91–124.
(40) Levin, E. M.; McDaniel, C. L. *J. Am. Ceram. Soc.* **1962**, *45*, 355–360.
(41) Egorysheva, A. V.; Burkov, V. I.; Kargin, Yu. F.; Plotnichenko, V. G.; Koltashev, V. V. *Crystallogr. Rep.* **2005**, *50*, 127–136.
(42) Henry, N.; Evain, M.; Deniard, P.; Jobic, S.; Abraham, F.; Mentré, O. *Z. Naturforsch.* **2005**, *60b*, 322–327.
(43) Grice, J. D. *Can. Mineral.* **2002**, *40*, 693–698.